Motile Properties of Vimentin Intermediate Filament Networks in Living Cells

Miri Yoon, Robert D. Moir, Veena Prahlad, and Robert D. Goldman

Northwestern University Medical School, Department of Cell and Molecular Biology, Chicago, Illinois 60611

Abstract. The motile properties of intermediate filament (IF) networks have been studied in living cells expressing vimentin tagged with green fluorescent protein (GFP-vimentin). In interphase and mitotic cells, GFP-vimentin is incorporated into the endogenous IF network, and accurately reports the behavior of IF. Time-lapse observations of interphase arrays of vimentin fibrils demonstrate that they are constantly changing their configurations in the absence of alterations in cell shape. Intersecting points of vimentin fibrils, or foci, frequently move towards or away from each other, indicating that the fibrils can lengthen or shorten. Fluorescence recovery after photobleaching shows that bleach zones across fibrils rapidly recover their fluorescence. During this recovery, bleached zones frequently move, indicating translocation of fibrils. Intriguingly, neighboring fibrils within a cell can exhibit different rates and directions of movement, and they often appear to extend or elongate into the peripheral regions of the cytoplasm. In these same regions, short filamentous structures are also seen actively translocating. All of these motile properties require energy, and the majority appear to be mediated by interactions of IF with microtubules and microfilaments.

Key words: intermediate filaments • vimentin • microtubules • microfilaments • green fluorescent protein

---

Iɴᴛᴇʀᴍᴇᴅɪᴀᴛᴇ filaments (IF)[1] are major cytoskeletal components of mammalian cells that appear to be relatively stable structures because of their insolubility in vitro and the lack of biochemical evidence for the existence of significant pools of soluble subunits in vivo (Steinert et al., 1976; Zackroff and Goldman, 1979; Soellner et al., 1985). However, there is increasing evidence that intermediate filaments are dynamic structures in vivo. For example, they form juxtanuclear aggregates in response to microinjection of IF antibodies and heat shock (Klymkowsky, 1981; Collier et al., 1993). In mitosis, partial or complete disassembly of IF networks takes place, followed by their reassembly in daughter cells (Franke et al., 1982; Rosevear et al., 1990). Furthermore, the state of IF polymerization is regulated by subunit exchange in vivo as suggested by the findings that microinjected vimentin and keratin, as well as newly synthesized IF proteins, become incorporated into preexisting IF networks (Vikstrom et al., 1989; Albers and Fuch, 1989; Ngai et al., 1990; Miller et al., 1993). The most direct evidence supporting an equilibrium between unpolymerized IF subunits and polymerized IF in vivo has been obtained from fluorescence recovery after photobleaching (FRAP) analyses (Vikstrom et al., 1992; Okabe et al., 1993).

Interactions of IF with IF-associated proteins (IFAPs), microtubules (MT), and microfilaments (MF) are thought to regulate IF organization in vivo (Chou et al., 1997). Structural evidence for IF–MT interactions comes from the observation of close parallel arrays of IF and MT, as well as the reorganization of IF to form perinuclear caps in response to MT depolymerization (Goldman and Knipe, 1973). Furthermore, MAP-2 (Hirokawa et al., 1988) and the IFAP plectin (Svitkina et al., 1996) have been shown to form cross-bridges between IF and MT. Evidence supporting IF–MF interactions comes from ultrastructural observations demonstrating close associations between IF and MF (Schliwa and van Blerkom, 1981), and from the finding that colcemid-induced movement of vimentin IF into perinuclear caps is inhibited by cytochalasin D (Hollenbeck et al., 1989). Candidates for cross-bridging elements between IF and MF include plectin and dystonin/BPAG1n (Brown et al., 1995; McLean et al., 1996; Yang et al., 1996).

Very little is known about the motile properties of IF due primarily to the difficulties inherent in visualizing IF

Address all correspondence to Robert D. Goldman, Northwestern University Medical School, Department of Cell and Molecular Biology, 303 E. Chicago Ave., Chicago, IL 60611. Tel.: 312-503-4215. Fax: 312-503-0954. E-mail: r-goldman@nwu.edu

1. *Abbreviations used in this paper*: GFP, green fluorescent protein; IF, intermediate filaments; MT, microtubules; MF, microfilaments; FRAP, fluorescence recovery after photobleaching; $t_{1/2}$, recovery half-time.

in vivo. Recently, many of these difficulties have been alleviated by expression of proteins tagged with the green fluorescent protein (GFP; Cubitt et al., 1995). Direct observations of GFP-tagged cytoskeletal proteins in vivo have provided insights into the dynamic properties of MT, MAP-4, actin, and IF (Olson et al., 1995; Ludin and Matus, 1998; Fischer et al., 1998; Ho et al., 1998).

In this study we describe in detail the motile properties of vimentin IF using GFP fused with vimentin (GFP-vimentin). After transfection with GFP-vimentin, time-lapse and FRAP analyses show that IF networks constantly change their configurations in vivo. GFP-vimentin fibrils are motile; they can translocate, alter their shapes, and apparently extend and shorten over relatively short time intervals. Time-lapse imaging of GFP-vimentin at the cell periphery reveals unexpected movement of short filamentous structures (termed squiggles). The effects of nocodazole and cytochalasin B indicate that many, but not all of these motile properties of IF are dependent on MT and/or MF.

Materials and Methods

Cloning of GFP-vimentin cDNA Constructs

A GFP-vimentin construct was made by fusing GFP to the NH_2-terminus of human vimentin cDNA. A BamHI–BamHI fragment containing the human vimentin cDNA sequence, with or without the human *c-myc* tag (Chou et al., 1996) was subcloned into the BamHI site of pEGFP-C1 (CLONTECH Laboratories Inc., Palo Alto, CA). The results obtained in cells transfected with GFP-vimentin with or without the *c-myc* tag were identical.

Cell Cultures and Transient Transfection

Baby hamster kidney (BHK-21) fibroblasts were grown in DME supplemented with 10% tryptose phosphate broth (Difco Laboratories Inc., Detroit, MI), 10% calf serum, and antibiotics (100 U/ml penicillin and streptomycin). SW13 vim$^-$ cells (a gift of Dr. Robert Evans, University of Colorado) were grown in DME with 10% FCS and antibiotics. Bovine pulmonary arterial endothelial cells (CPAE; American Type Culture Collection, Rockville, MD) were grown in DME with 2 mM glutamine, 10% FCS, and antibiotics. HeLa and PtK2 cells were grown in MEM with 10% FCS, 0.1 mM nonessential amino acid solution (GIBCO-BRL, Gaithersburg, MD), and antibiotics.

For transfection, Lipofectamine™ (GIBCO-BRL) was used according to the manufacturer's protocol. Cells grown on coverslips were incubated with a mixture of 1 μg of CsCl-purified DNA and 6 μl of Lipofectamine™ in serum-free medium for 3 h, after which the mixture was replaced with standard culture medium.

Preparation of IF-enriched Cytoskeletons and Immunoprecipitation

IF-enriched cytoskeletal preparations were made from confluent BHK-21 cell cultures (Zackroff and Goldman, 1979), and the final pellet was solubilized and sonicated in 10 mM Tris-HCl, pH 6.8, 5 mM EDTA, 2% SDS, 10% glycerol, and Complete™ protease inhibitors (Boehringer Mannheim Corp., Indianapolis, IN). The resulting solution was diluted 1:20 in 20 mM Tris-HCl, pH 7.5, 150 mM NaCl, 1% NP-40, 5 mM EDTA, and Complete™ protease inhibitors, and was used for immunoprecipitation experiments.

Immunoprecipitation of GFP-vimentin was carried out with Protein A-sepharose (Sigma Chemical Co., St. Louis, MO) and 9E10, a mouse monoclonal anti-human *c-myc* antibody (Evan et al., 1985; American Type Culture Collection) as described elsewhere (Chou et al., 1990). The immunoprecipitates were separated by SDS-PAGE (Laemmli, 1970). Immunoblotting was carried out according to Towbin et al. (1979). The primary antibodies used were 9E10 and a mouse monoclonal anti-vimentin (Sigma Chemical Co.). The secondary antibody used was peroxidase-conjugated goat anti-mouse IgG (Jackson ImmunoResearch Laboratories Inc., West Grove, PA).

Indirect Immunofluorescence

Cells grown on coverslips were fixed and processed for indirect immunofluorescence as described by Yang et al. (1985). The primary antibodies used were 9E10, a rabbit polyclonal anti-BHK IF (Yang et al., 1985), a rabbit polyclonal anti-bovine tongue keratin antibody (Jones et al., 1988) and a mouse monoclonal anti-β-tubulin (Amersham Life Science, Inc., Arlington Heights, IL). The secondary antibodies used were fluorescein-conjugated goat anti–mouse IgG and Lissamine rhodamine (LRSC)-conjugated donkey anti-rabbit IgG (Jackson ImmunoResearch Laboratories, Inc.).

Microscopy

For live cell studies, transfected cells were trypsinized 48 h after transfection, and were plated onto coverslips to achieve 70% confluence in standard culture medium containing 10 mM Hepes, pH 7.0. The coverslips were placed on small glass feet (to prevent compression) on slides, sealed with a mixture of Vaseline, beeswax, and lanolin (1:1:1), and maintained at 37°C with an air stream stage incubator (Model ASI 400; NEVTEK, Burnsville, VA). In some cases, these coverslips were treated with nocodazole (Sigma Chemical Co.) at final concentrations of either 100 or 600 nM. In other cases, cytochalasin B (Sigma Chemical Co.) was added at final concentrations of either 2 or 20 μM. For metabolic inhibition studies, final concentrations of both 50 mM 2-deoxy-D-glucose (Sigma Chemical Co.) and 0.05% sodium azide (Sigma Chemical Co.) were added. For cell-cycle studies, chromosomes were stained with 2 μg/ml of Hoechst 33258 (Molecular Probes Inc., Eugene, OR).

Time-lapse observations were made with an LSM 410 confocal microscope (Carl Zeiss, Inc., Thornwood, NY) equipped with a 100×, 1.4 NA oil immersion objective. Phase-contrast images of cells were taken before and after time-lapse observations to ensure that no significant change in cell shape or position occurred during the periods of observation. Digitized images were collected every 30 s for 30–40 min using a fluorescein filter set (excitation at 488 nm and emission at 515–560 nm). To test the stability of the focal plane in the confocal microscope, we made time-lapse observations of MT patterns for 30 min in fixed BHK cells after staining with anti-β-tubulin. No obvious change in focus was detected during this time interval. This minimized problems due to focal plane drift during the periods of observation.

In some cases, indirect immunofluorescence observations were made using a Zeiss Axiophot with a CCD camera (Photometrics, Tucson, AZ) controlled by Metamorph imaging software (Universal Imaging Corp., West Chester, PA).

Fluorescence Recovery After Photobleaching (FRAP)

FRAP was carried out with the LSM 410 confocal microscope (Carl Zeiss, Inc., Thornwood, NY). Phase-contrast images of cells were taken before and immediately after FRAP to ensure that there were no significant changes in cell shape or position. Bar-shaped regions were bleached using the line-scan function at 488 nm (100% power, 1% attenuation), and recovery of fluorescence was monitored (15–30% power, 10% attenuation) using the time-series function at 2-min intervals for up to 1 h.

Image Analyses

Position, length, and intensity measurements were made on digitized confocal images using Metamorph image analysis software. Pixel values were converted to distance using confocal calibration bars. Analyses of the dynamic properties of GFP-vimentin fibrils were restricted to cells that showed no obvious shape changes for 30–40 min. If the average displacement of a cell's margins was more than 2 μm in 40 min (0.05 μm/min) as indicated by phase contrast, it was excluded from the analyses. Rates of translocation of vimentin fibrils were determined by monitoring distance vs. time. If vimentin fibrils or foci moved at least 0.25 μm in 5 min (0.05 μm/min), the data were used to calculate the rates of movements.

FRAP half-times ($t_{1/2}$) were calculated by monitoring the gray-scale pixel values (intensity measurements) across the bleached vimentin fibrils using the line-scan function of Metamorph at each time point after adjustment for sample fading during time-lapse observations (see Vikstrom et al., 1992). All data are reported as mean ± SD.

Results

Characterization of the GFP-vimentin Fusion Protein In Vivo and In Vitro

GFP-vimentin was expressed in ∼30% of the BHK-21 cells 72 h after transfection. The majority of these cells dis-
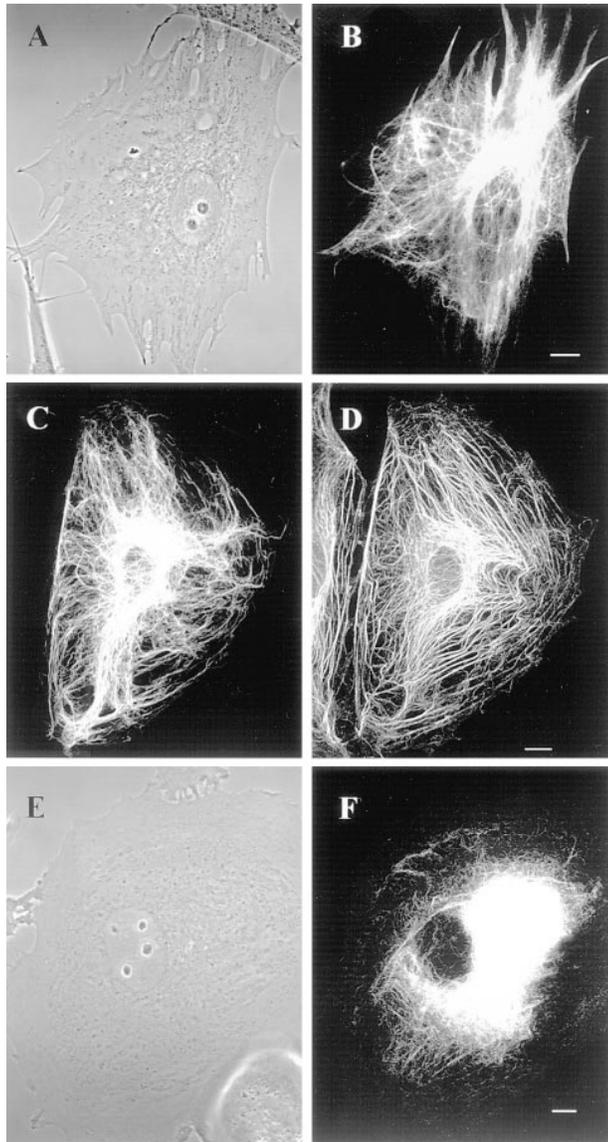

Figure 1. GFP-vimentin IF networks in interphase cells 72 h after transfection. (*A* and *B*) Phase-contrast (*A*) and fluorescence (*B*) images of a live BHK cell show that GFP-vimentin IF networks extend from the perinuclear region to the cell periphery. (*C* and *D*) In PtK2 cells that contain vimentin and keratin IF networks, GFP-vimentin is incorporated into the vimentin IF network, as indicated by fixation and double indirect immunofluorescence. GFP-vimentin-*myc* (*C*) was visualized with monoclonal anti-human *c-myc* antibody and keratin (*D*) with polyclonal anti-bovine tongue keratin antibody. (*E* and *F*) Phase-contrast (*E*) and GFP (*F*) images of a live BHK cell after treatment with 600 nM nocodazole for 5 h. The majority of the vimentin IF network is reorganized into a perinuclear cap. Bar, 5 μm.

played typical cytoplasmic IF networks (Fig. 1, *A* and *B*), indistinguishable from those seen by immunofluorescence (Yang et al., 1985). GFP-vimentin colocalized with endogenous vimentin as demonstrated by double-label immunofluorescence (see Fig. 6, *B*, and *E–F*). GFP-vimentin also formed typical IF networks in CPAE endothelial cells (see Fig. 5). In HeLa (data not shown) and PtK2 cells that have two IF networks, GFP-vimentin was incorporated only into the vimentin and not the keratin IF network (Fig. 1, *C* and *D*). GFP-vimentin does not appear to alter the properties of interphase IF networks as indicated by observations such as their reorganization into a perinuclear cap after the disassembly of MT (Fig. 1, *E* and *F*; see Yang et al., 1992).

To ensure further that transfected cells accurately display the properties of IF, the cell cycle–dependent behavior of GFP-vimentin was studied in live cells. In mitotic BHK-21 cells, the fluorescent IF networks disassembled into nonfilamentous aggregates (Fig. 2, *A*, *B*, *D*, and *E*), and during cytokinesis reassembled into a juxtanuclear cap in each daughter cell (Fig. 2, *C* and *F*). These observations are very similar to those seen by immunofluorescence (Rosevear et al., 1990). In PtK2 cells, GFP-vimentin IF aggregated around the mitotic spindle (Fig. 2, *G*, *H*, *J*, and *K*), and were distributed to daughter cells in cytokinesis coincident with a loss of fluorescence in the midbody region (Fig. 2, *I* and *L*). This was also identical to the results obtained by immunofluorescence (Aubin et al., 1980). Therefore, GFP-vimentin follows the normal progression of changes of IF during cell division and acts as a faithful reporter of IF in live cells.

We have also attempted to establish GFP-vimentin IF networks in cells lacking vimentin. To this end, SW13 vim⁻ cells were transfected with GFP-vimentin. Under these conditions, ∼4–5% of the cells expressed GFP-vimentin. However, only 1% of these displayed typical IF patterns, while the remainder displayed only aggregates of vimentin (data not shown; see Ho et al., 1998). This low level of expression of typical IF networks may be related to the leaky expression of vimentin that we detected in ∼1% of SW13 vim⁻ cells. Furthermore, when these vim⁻ cells were cotransfected with wild-type vimentin (Chou et al., 1996) and GFP-vimentin, 20% of the cells displayed typical IF networks (data not shown). These results indicate that GFP-vimentin is capable of assembling into IF only in the presence of a wild-type background.

GFP-vimentin with the *c-myc* tag was tested at the biochemical level for its ability to incorporate into endogenous IF networks in BHK-21 cells. 72 h after transfection, IF-enriched cytoskeletons were prepared from cultures with ∼30% transfected cells. SDS-PAGE analyses indicated the presence of vimentin, other IF-associated proteins, and a minor 82-kD band corresponding to the molecular weight of GFP-vimentin (Fig. 3 *A*). Immunoblot analyses of these preparations showed that the 82-kD band reacted with *c-myc* antibody (Fig. 3 *B*). These cytoskeletal preparations were also solubilized, immunoprecipitated with *c-myc* antibody, and analyzed by SDS-PAGE and immunoblotting. The results showed a single band of 82 kD recognized by *c-myc* antibody (Fig. 3 *C*), and both the 82-kD fusion protein and 55-kD untagged vimentin with vimentin antibody (Fig. 3 *D*). These results
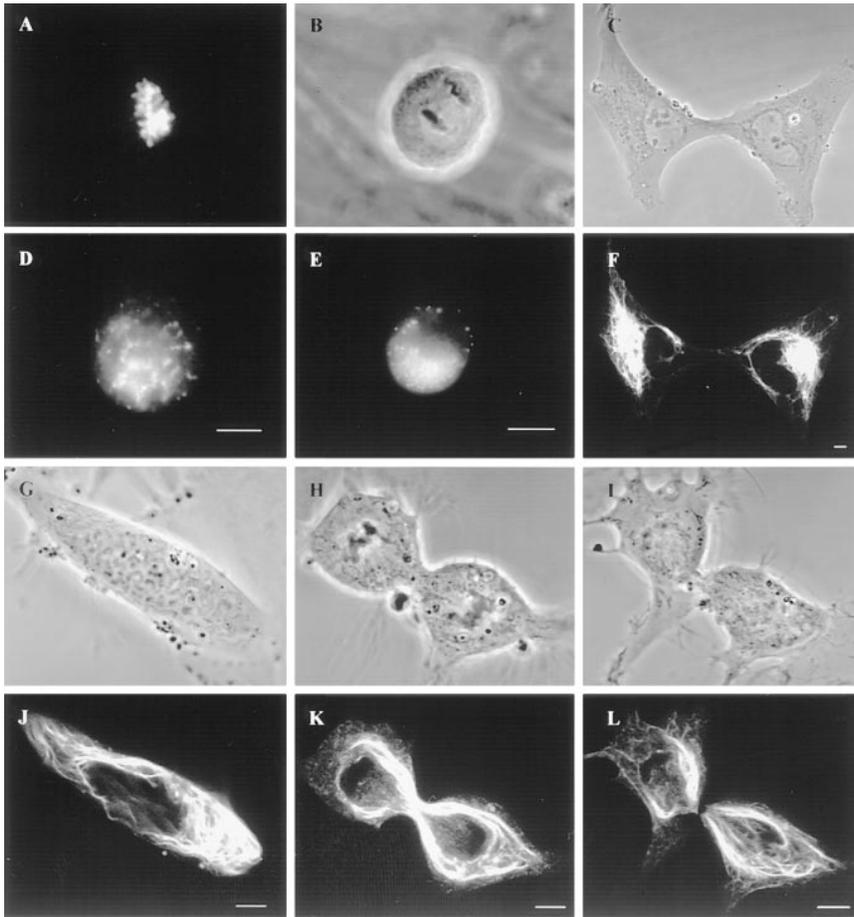
Figure 2. Dynamic properties of GFP-vimentin in live cells during mitosis. (*A–F*) Mitotic BHK-21 cells. BHK cell in prometaphase showing chromosomes stained with Hoechst-33258 (*A*) and GFP-vimentin nonfilamentous aggregates (*D*). Phase-contrast (*B*) and fluorescence (*E*) images in anaphase. Phase-contrast (*C*) and GFP (*F*) images show reassembly into juxtanuclear caps in two daughter cells. (*G–L*). Phase-contrast (*G*, *H*, and *I*) and fluorescent (*J*, *K*, and *L*) images of PtK2 cells showing the cage-like structure of vimentin fibrils during pro-metaphase (*G* and *J*), telophase (*H* and *K*) and in late cytokinesis (*I* and *L*). Note the loss of fluorescence in the region of the midbody in *L*. *L* is the same cell as *K*, taken 10 min later. Bar, 5 μm.

provide further support that GFP-vimentin is incorporated into the endogenous IF network.

Time-lapse Observations of GFP-vimentin IF Networks in Interphase Cells

Time-lapse observations of GFP-vimentin IF networks were made in well-spread BHK-21 cells 72 h after trans-
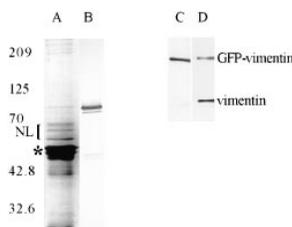

Figure 3. Analysis of an IF-enriched cytoskeletal preparation of BHK-21 cells 72 h after transfection with GFP-vimentin-*myc*. SDS-PAGE analysis (*A*) reveals the presence of vimentin/desmin (*) and other proteins that coisolate with IF such as the nuclear lamins (*NL*) as well as 82-kD GFP-vimentin-*myc*, which is detected by immunoblotting with *c-myc* antibody (*B*). When these preparations were solubilized and immunoprecipitated with the *c-myc* antibody, GFP-vimentin-*myc* as well as endogenous vimentin were found in the immunoprecipitates. *C* is an immunoblot of the immunoprecipitate using the *c-myc* antibody showing a single 82-kD band; and *D* shows a blot of the same preparation using a monoclonal antibody directed against vimentin (*V9*; Sigma Chemical Co.) showing both the 82-kD GFP-vimentin and 55-kD untagged vimentin.

fection. Details of changes in the morphological features of GFP-vimentin IF networks were determined by time-lapse recording at 30-s intervals for 30–40 min. Analyses were restricted to cells that showed no obvious shape changes, as determined from phase-contrast images taken before and at the end of the time-lapse observations (see Materials and Methods). This procedure ensured that we were monitoring intrinsic changes in IF networks and not passive displacements due to significant changes in cell shape.

The fluorescent IF networks were characterized by extensive arrays of fibrils. In some cases, fibrils appeared to be interconnected at diffusely fluorescent focal points (foci). The majority of the vimentin fibrils and foci displayed movements during the periods of observation. These foci were useful indicators of motility as they frequently moved towards or away from each other (Fig. 4, *A–C*). The average rate of translocation of the foci and therefore changes in the length of the interconnecting fibrils was 0.42 ± 0.16 μm/min ($n = 21$). In no case did we observe a change in the direction of the movement of foci. However, this might be due to the limited time intervals of observation.

Other types of movements frequently seen included significant shape changes in fibrils, as indicated by bending and/or straightening (Fig. 4, *D–F*). Fibrils also appeared or disappeared in the focal plane (Fig. 4, *G–H*). In addition, numerous fibrils appeared to extend into regions contain-
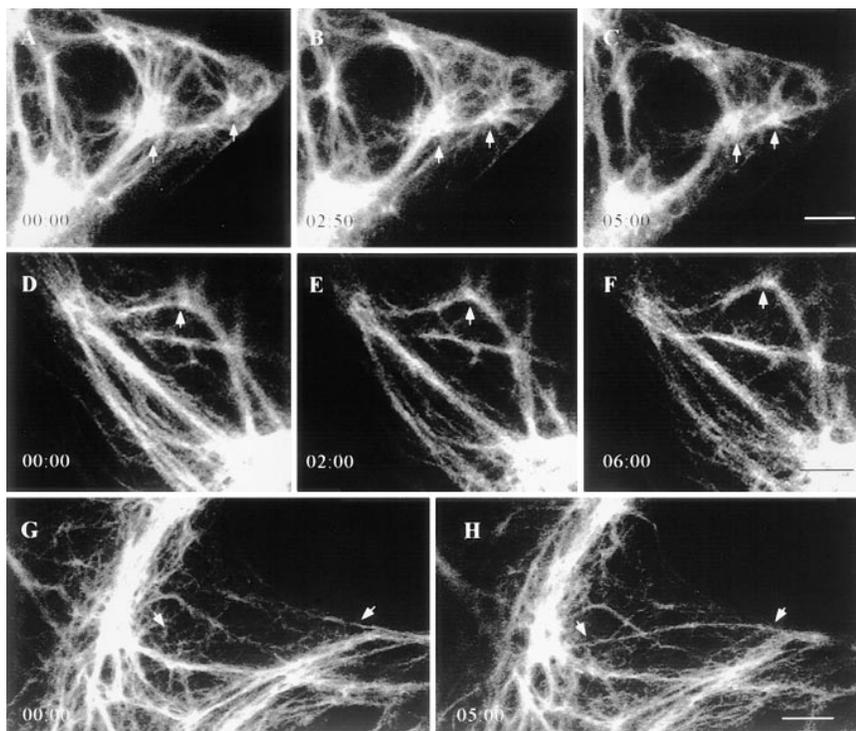
Figure 4. Time-lapse observations of GFP-vimentin IF networks in live BHK-21 cells. (*A–C*) GFP-vimentin fibrils often interconnect bright foci (*arrows*), and in this case, the foci move towards each other while the fibrils interconnecting these foci appear to shorten. (*D–F*) Vimentin fibrils can change their shapes, as indicated by bending (*arrows*). (*G–H*) GFP-vimentin fibrils often appear in the focal plane over relatively short time intervals (*arrows*). Lapsed time (*min:sec*) is indicated at lower left. Bar, 5 μm.

ing a few IF at the cell periphery. This was especially evident in the extremely thin edges of CPAE cells. The average rate of extension at the cell periphery was 1.7 ± 1.1 μm/min with a range of 0.4–4.4 μm/min ($n = 30$; Fig. 5, *A–I*).

FRAP Analyses

In our earlier FRAP studies, after microinjecting rhodamine-labeled vimentin, we showed that there is an equilibrium between unpolymerized vimentin IF subunits and
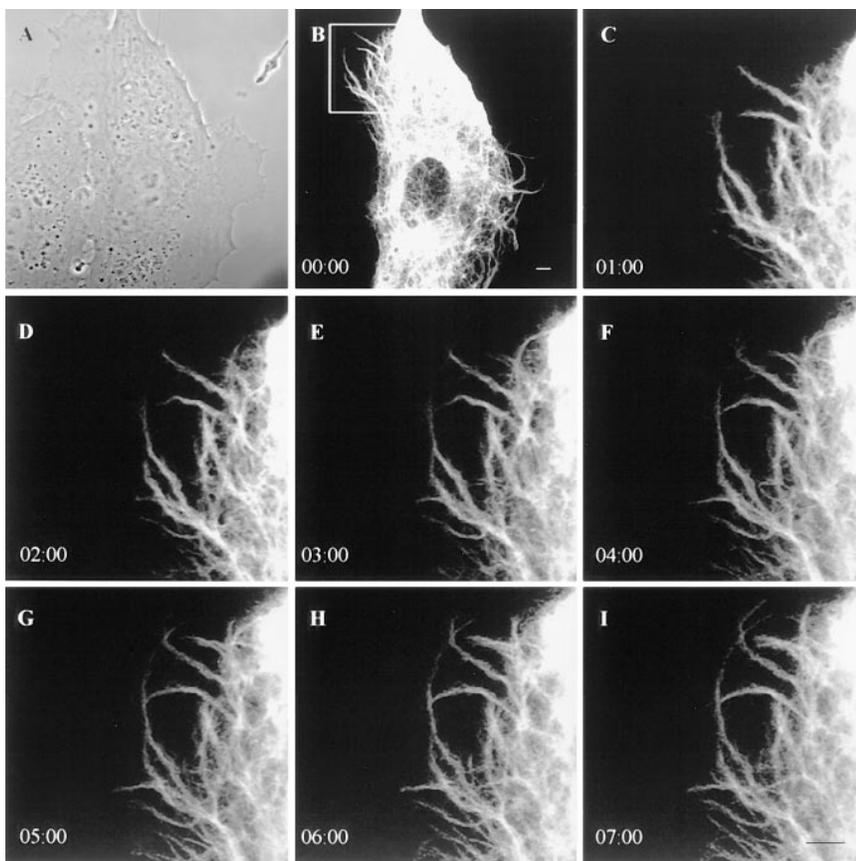

Figure 5. Time-lapse observations of GFP-vimentin fibrils in a live CPAE cell. Phase-contrast (*A*) and GFP images (*B–I*) indicate that GFP-vimentin fibrils extend into a region lacking IF at the edge of a cell. Intervals between frames are 1 min. Bar, 5 μm.
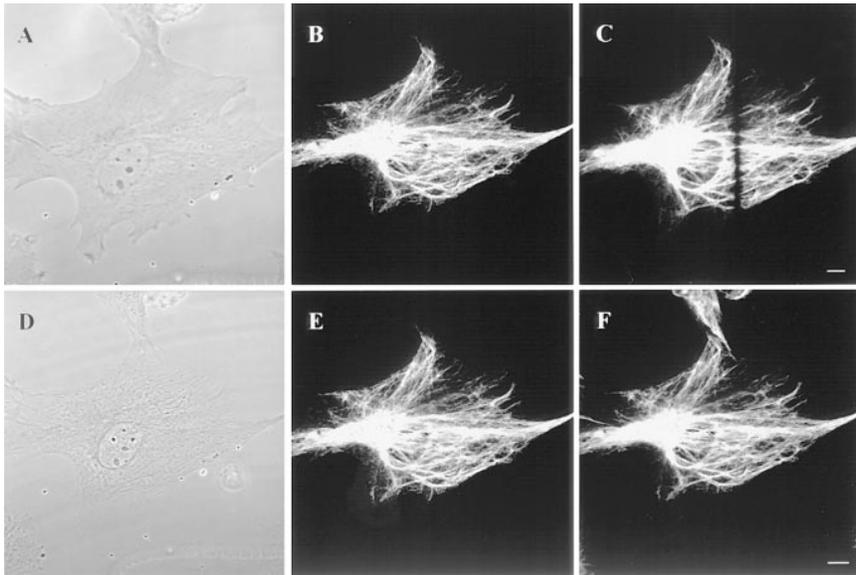
Figure 6. Continuity of vimentin fibrils across bleach zones following photobleaching. A GFP-vimentin-*myc* expressing BHK-21 cell was fixed at ~1 min after photobleaching, and was processed for indirect immunofluorescence. The continuous vimentin-staining pattern across the bleach zones indicates that photobleaching does not damage vimentin fibrils. (*A–C*) This series depicts a live cell in phase-contrast (*A*) and GFP before (*B*) and immediately after (*C*) photobleaching. (*D–F*) Phase-contrast image (*D*). GFP-vimentin (*E*) is visualized with *c-myc* antibody and vimentin (*F*) with a polyclonal BHK IF antibody (*F*) in the same cell after fixation and processing for double indirect immunofluorescence. Bar, 10 μm.

polymerized vimentin IF in vivo. The main drawback of our previous study was our inability to estimate the average recovery half-time ($t_{1/2}$) due to relatively rapid background photobleaching (Vikstrom et al., 1992). A major advantage of using GFP fusion proteins is that fluorescence intensity does not decrease significantly during image acquisition over relatively long periods (Cubitt et al., 1995). Since our observations suggested that many fibrils were motile (Figs. 4, 5), FRAP analyses also provided an-

other means of monitoring IF translocation during recovery, especially in regions of the cytoplasm containing parallel arrays of fibrils without a significant number of interconnecting foci.

To ensure that photobleaching did not damage vimentin IF in vivo, BHK cells expressing GFP-vimentin-*myc* were fixed 1 min after bleaching, and were processed for double indirect immunofluorescence (Fig. 6). The continuous vimentin-staining patterns across the bleach zones indicated
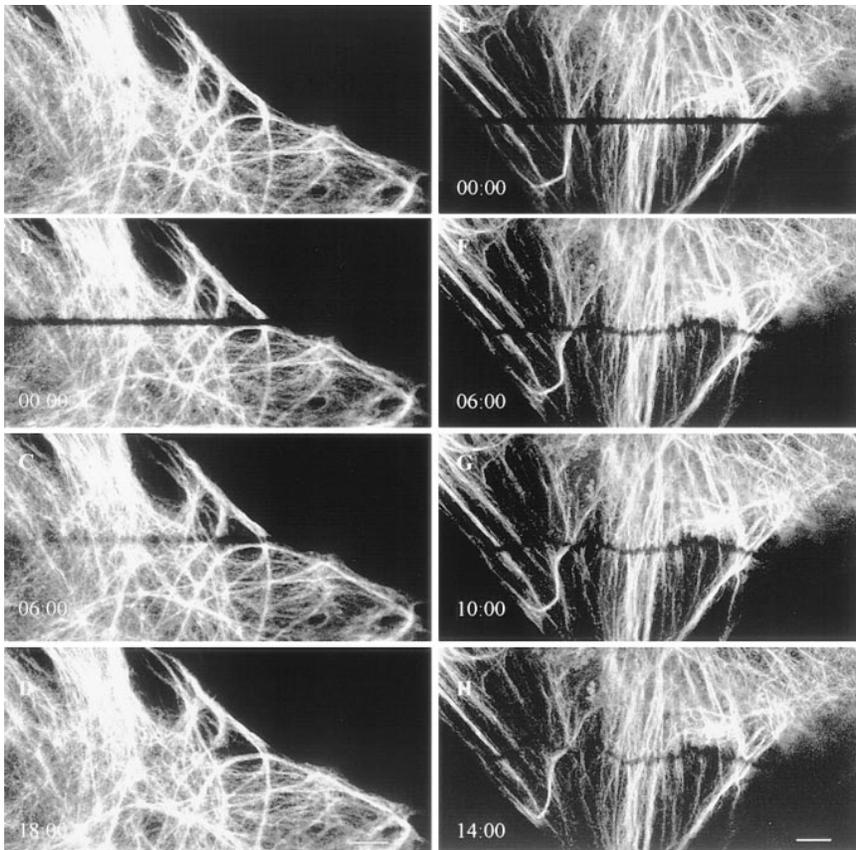

Figure 7. Time-lapse observations of FRAP in GFP-vimentin fibrils in a BHK-21 cell. (*A–D*) The bleached GFP-vimentin fibrils completely recover their fluorescence within 20 min. (*E–H*) Frequently the bleach zones on individual fibrils move at different rates during fluorescence recovery, as indicated by the transformation of the straight bleach zone into a wavy line. Lapsed time (*min:sec*) is indicated at the lower left of each image. Bar, 10 μm.
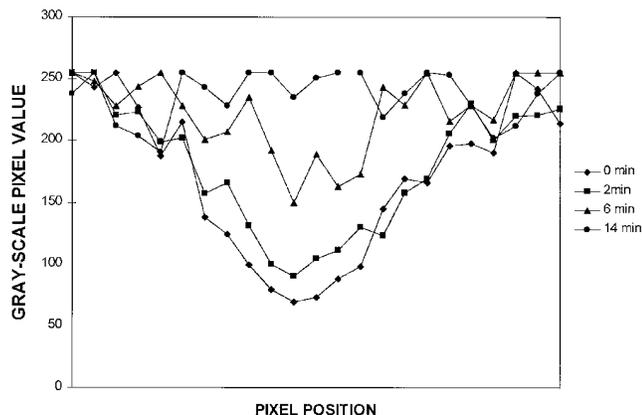
152

Figure 8. Fluorescence intensity measurements along a photobleached GFP-vimentin fibril. Gray-scale pixel values were determined along a bleached vimentin fibril every 2 min with the Metamorph image analysis program. In this case, complete recovery took place in 14 min with a recovery half-time ($t_{1/2}$) of ∼6 min.

that photobleaching did not disrupt the integrity of the vimentin fibrils.

Time-lapse observations were made at 2-min intervals for 60 min after photobleaching. In some cytoplasmic regions, bleach zones were relatively stationary during recovery (Fig. 7, *A–D*). FRAP analyses of such stationary fibrils indicated that the fluorescence intensities along bleached vimentin fibrils increased with time, and that no preferential recovery from either side could be detected (Fig. 8). The average time for the bleach zones to completely recover their fluorescence was 23 ± 12 min with an average $t_{1/2}$ of 5 ± 3 min ($n = 25$).

In many instances bleach zones across fibrils moved during recovery. Bleach zones on closely spaced parallel fibrils either moved towards the nucleus or in the opposite direction towards the cell surface (Fig. 7, *E–H*). This suggests that individual neighboring fibrils can translocate in-

dependently. The average rate of translocation of fibrils as determined from these motile bleach zones was 0.24 ± 0.14 μm/min ($n = 23$).

Motile Properties of Short Vimentin Fibrils

In addition to the typical networks of interconnecting fibrils seen in transfected cells, short filamentous structures termed vimentin squiggles were frequently visible. These were most apparent in the thin peripheral regions of BHK-21 cells (Fig. 9, *A–F*). Vimentin squiggles were also seen in fixed untransfected BHK-21 and PtK2 cells (data not shown).

Time-lapse observations of these squiggles showed that the majority were motile. Of 269 squiggles monitored for 10 min or more, 237 moved a distance of at least 0.5 μm ($237/269 = 88\%$). The majority of the motile squiggles ($231/237 = 97\%$) moved towards the cell periphery. In some cases, squiggles reached the edge of the cell where they altered their shapes to reorient and move parallel to the cell surface (Fig. 9, *D–F*). Squiggles translocated at speeds ranging from 1.3 to 11.4 μm/min ($n = 32$), with an average rate of 3.3 ± 1.9 μm/min in BHK-21 cells. It should be noted that squiggles frequently underwent shape changes, even when they were not translocating.

Nocodazole Treatment Affects the Motile Properties of IF

Low concentrations of nocodazole (e.g., 100 nM) are known to interfere with MT dynamics without significantly affecting the number or distribution of MT (Liao et al., 1995; Vasquez et al., 1997). The overall distributions of MT and IF in BHK-21 cells treated with 100 nM nocodazole for 30–60 min were similar to those of untreated cells as determined by fixation and double indirect immunofluorescence (data not shown). To determine whether the motile properties of GFP-vimentin fibrils in vivo were dependent on MT dynamics, we carried out time-lapse observations and FRAP analyses after adding 100 nM nocodazole for 30 min. Vimentin-rich foci continued to move
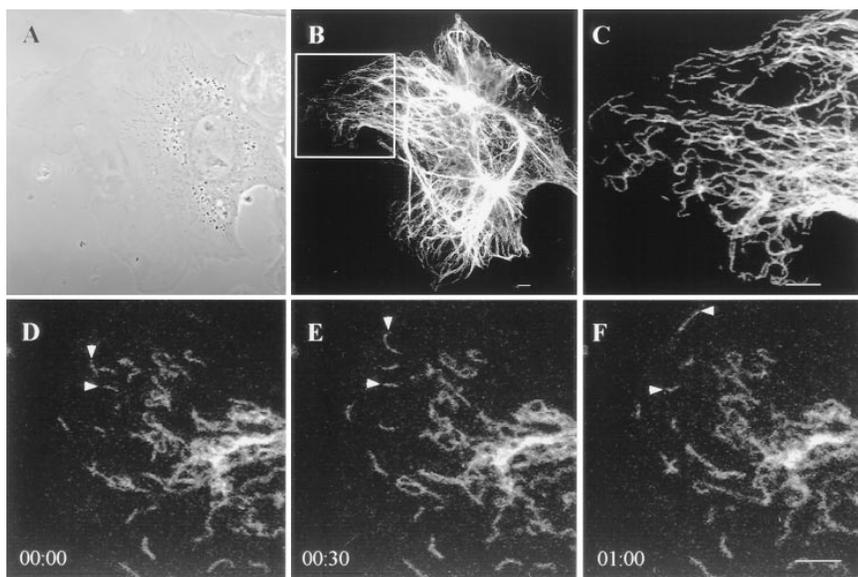

Figure 9. Vimentin squiggles in live BHK-21 cells. (*A–C*) Phase-contrast (*A*) and fluorescence (*B* and *C*) images showing that squiggles are present in the peripheral region of the same cell. (*D–F*) Time-lapse observations demonstrating that the majority of vimentin squiggles are motile. The squiggle indicated by the top arrow shows a bending movement and a change of direction at the cell surface. Time intervals between frames are 30 s. Bar, 5 μm.
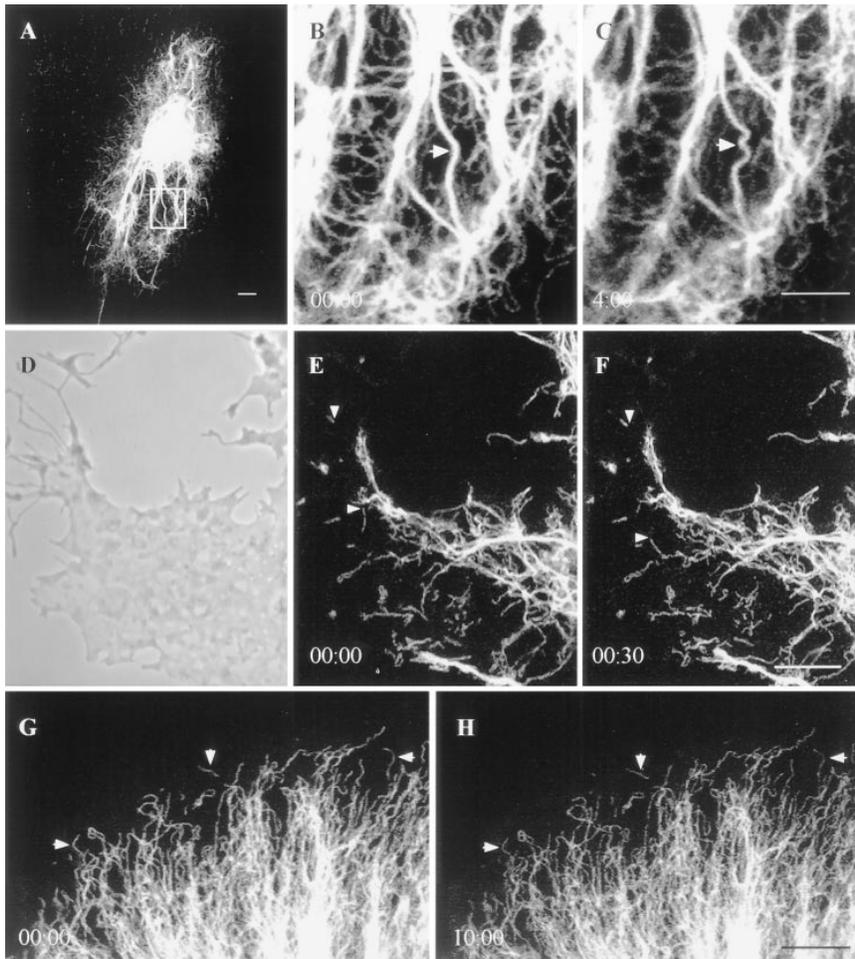
Figure 10. GFP-vimentin in live BHK-21 cells treated with nocodazole, cytochalasin B, and metabolic inhibitors. (*A*) Cell treated with 600 nM nocodazole for 5 h. Note that the majority of vimentin fibrils are reorganized into a perinuclear cap, but that some fibrils remain associated with the cell surface. (*B* and *C*) Nocodazole-insensitive fibrils seen in *A* at higher magnification to show that shape changes continue in the absence of microtubules. (*D*) Phase-contrast image of the edge of a cell 30 min after the addition of 20 μM cytochalasin B. Cell margins have retracted and the overall morphology becomes arborized. (*E* and *F*) GFP-vimentin squiggles are present in the same region of this cell. Two squiggles (*arrows*) showing translocations in the 30-s interval between these two images. (*G* and *H*) Motility of GFP-vimentin fibrils is completely arrested 15 min after adding 50 mM 2-deoxy-D-glucose and 0.05% sodium azide. This is most obvious when observing squiggles at the edge of a cell (see *arrows*). Lapsed time (*min:sec*) is indicated at lower left of figures. Bar, 5 μm.

relative to each other, and the fibrils interconnecting them appeared to shorten or lengthen at an average rate of 0.18 ± 0.06 μm/min ($n = 16$), representing a decrease of 58% compared with control cells. Fibrils also continued to change their shapes under these experimental conditions. FRAP analyses indicated that fibrils recovered their fluorescence more slowly at a $t_{1/2}$ of 8 ± 5 min ($n = 16$). During recovery, some bleach zones moved at an average rate of 0.14 ± 0.09 μm/min ($n = 22$), a 43% decrease relative to control cells. At the cell periphery, 93% (296/318) of the squiggles translocated at an average rate of 3.4 ± 1.6 μm/min ($n = 16$), ranging from 1.5 to 9.9 μm/min, which was similar to controls. We also studied fibril extension at the edges of endothelial cells in this concentration of nocodazole and found the average rate was 1.6 ± 0.7 μm/min ($n = 20$), which was also similar to controls.

When BHK cells were treated with 600 nM nocodazole for 5 h, MT depolymerized (data not shown), and the majority of vimentin IF reorganized into perinuclear caps (Fig. 1, *E*–*F*). Under these conditions, some vimentin fibrils remained extended towards the cell periphery, and squiggles could be found near the cell surfaces; however, it was difficult to locate foci (Fig. 10 *A*; see Yang et al., 1992). Time-lapse observations showed that the extended fibrils continued to change their shapes (Fig. 10, *B* and *C*), and FRAP analyses showed that they recovered their fluo-

rescence more slowly at a $t_{1/2}$ of 8 ± 3 min ($n = 12$). During recovery, some bleach zones moved at a rate of 0.1 ± 0.07 μm/min ($n = 7$), representing a 60% decrease compared with controls. The majority of vimentin squiggles (381/400 = 95%) did not move during the periods of observation. However, 5% of the squiggles continued to move at a rate of 3 ± 1.9 μm/min ($n = 19$; range 0.4–8.9 μm/min), which was similar to controls.

Inhibition of Actin Function Affects IF Motility

Cytochalasin B was used to determine whether vimentin motility was dependent on MF. It has been shown that 2 μM cytochalasin B inhibits actin-related functions such as membrane ruffling and cell locomotion without significantly affecting cell shape or the overall distribution of IF, MF, or MT (Goldman and Knipe, 1973). After treatment with 2 μM cytochalasin B for 30 min in GFP-vimentin–transfected BHK-21 cells, foci moved at an average rate of 0.18 ± 0.09 μm/min ($n = 12$), a 58% decrease relative to controls. FRAP analyses demonstrated a complete, although somewhat slower recovery with a $t_{1/2}$ of 10 ± 5 min ($n = 17$). During recovery, some bleach zones moved at an average rate of 0.15 ± 0.08 μm/min ($n = 13$), a 38% decrease compared with controls, while the majority (134/163 = 82%) of the squiggles continued to translocate at a

rate similar to controls (3.4 ± 1.5 μm/min, *n* = 19; range 1.5–7.2 μm/min).

When transfected cells were exposed to 20 μM cytochalasin B for 30 min, BHK-21 cell margins retracted, and the overall morphology became arborized (Fig. 10 *D*; see Goldman and Knipe, 1973). FRAP analyses showed complete but slower recovery with a $t_{1/2}$ of 11 ± 5 min (*n* = 12). Some bleach zones moved at 0.09 ± 0.04 μm/min (*n* = 7), a 60% decrease compared with controls, and squiggles continued to translocate (92/105 = 88%) at an average rate of 3.3 ± 2.4 μm/min (*n* = 17; range 0.4–6.4 μm/min; Fig. 10, *D–F*), again similar to controls. Shape changes of fibrils and squiggles were seen at both concentrations of cytochalasin B (data not shown).

The Motile Properties of IF Require Metabolic Energy

To determine whether ATP is required for the motile properties of IF, we made time-lapse observations of GFP-vimentin IF networks after treating BHK-21 cells with 50 mM 2-deoxy-D-glucose and 0.05% sodium azide for 30 min (Donaldson et al., 1990). None of the movements described above were detected over time periods of up to 40 min after 30 min of pretreatment with these inhibitors (Fig. 10, *G–H*). These results demonstrate that the motile properties of vimentin IF require metabolic energy.

Discussion

The overall organization of IF networks containing GFP-vimentin in several types of live cells during interphase, mitosis, and exposure to nocodazole were indistinguishable from those seen by immunofluorescence in nontransfected cells. Immunoblot and immunoprecipitation analyses of transfected cells indicated that a portion of endogenous vimentin formed stable complexes with the 82-kD GFP-vimentin. The nature of these complexes is unknown, but the solubilization conditions used for our immunoprecipitation assays suggest that these complexes represent dimers or tetramers containing endogenous and GFP-vimentin. These results, in addition to the FRAP observations, reassure us that the previously described properties of vimentin IF are retained after transfection, and that GFP-vimentin is a faithful reporter of the dynamic properties of IF in living cells.

The Motile Properties of Vimentin IF

Time-lapse observations of interphase cells expressing GFP-vimentin showed that fibrils exhibit numerous types of motility. For example, fibrils frequently appeared and disappeared in the same focal plane in the thin sheets of cytoplasm at the cell periphery. It is possible that these IF fibrils were moving in or out of the plane of focus. However, it is also possible that these observations represent local assembly or disassembly of IF (also see Prahlad et al., 1998). We also observed apparent fibril extension in the peripheral regions of cells. However, at the present time we cannot determine whether this extension of fibrils is due to active growth and elongation of fibrils or to the movement of preexisting fibrils due to sliding with respect to other cytoskeletal components such as MT and/or MF.

Vimentin fibrils also appeared to be capable of lengthening and shortening as evidenced by the movement of interconnected foci either towards or away from each other. Movements of parallel arrays (not interconnected by foci) of vimentin fibrils were also observed due to the movements of bleach zones. Interestingly, both of these types of IF motility are sensitive to nocodazole and cytochalasin B, indicating a dependence on both MT and MF network integrity. It should be noted that there is evidence that the movement of IF towards the nucleus is MF dependent (Hollenbeck et al., 1989), and that their movement towards the cell surface is MT-dependent. The latter dependency appears to be related to a kinesin motor activity (Gyoeva and Gelfand, 1991; Prahlad et al., 1998).

Short filamentous structures with two free ends, vimentin squiggles (also see Osborn, 1980; Prahlad et al., 1998), exhibited rapid movements, primarily towards the edge of cells at speeds up to 11 μm/min. Squiggles continued to translocate at the same rates as controls in the presence of cytochalasin B. However, only ~5% of the squiggles moved at the same rates as controls in the absence of MT. These observations suggest that translocation of the vast majority of squiggles is dependent on MT, most likely through MT-associated motor molecules such as kinesin. The observation that a small number of squiggles continue to translocate in the absence of MT is intriguing, and suggests that the motility of a subpopulation may be dependent on either MF and their associated proteins or unknown factors. In support of the former possibility, IF have been shown to interact with MF, and proteins have been identified that can form cross-bridges between these two cytoskeletal systems (Brown et al., 1995; McLean et al., 1996; Yang et al., 1996).

It is also interesting to compare the rates of movement of bleach zones and photoactivated fluorescent marks along MT and MF with the rates obtained for IF in this study. For MT, analyses of mitotic and interphase MT bleach zones have revealed rates of 0.1–0.7 μm/min (Gorbsky and Borisy, 1989; Mitchison, 1989; Waterman-Storer and Salmon, 1997). Bleach zones made across microspikes containing fluorescent MF moved at 0.79 ± 0.31 μm/min (Wang, 1985), and in stress fibers the rates were 0.29 ± 0.1 μm/min (McKenna and Wang, 1986). Therefore, the rate of translocation of bleach zones on vimentin fibrils is similar to the rates recorded for MT and MF, irrespective of the differences in the mechanisms responsible for these movements (i.e., treadmilling for MT and MF). Intriguingly, adjacent vimentin fibrils move either towards or away from the cell center at different speeds while other fibrils in neighboring cytoplasmic regions remain stationary. These observations are different from the unidirectional movements of bleached zones toward the nucleus thus far reported for interphase MT and MF (McKenna and Wang, 1986; Waterman-Storer and Salmon, 1997).

Vimentin fibrils frequently changed their shapes as evidenced by bending or straightening movements within short time intervals. These movements continued in the presence of nocodazole and cytochalasin B, suggesting that they represent intrinsic motile properties of IF independent of MT and MF. Interestingly, metabolic inhibitors completely arrested these shape changes, demonstrating that these movements require energy.

Use of GFP-vimentin To Monitor Subunit Exchange In Vivo

Using GFP-vimentin in FRAP analyses has permitted us to calculate accurately a recovery half-time ($t_{1/2}$) of 5 ± 3 min in BHK-21 cells. Similar analyses of interphase MT have indicated a $t_{1/2}$ of 4.5 ± 1.2 min in PtK1 cells, and 3.3 ± 1.4 min in BSC cells (Saxton et al., 1984). In the case of actin in stress fibers, a $t_{1/2}$ of 5–10 min has been reported (Kreis et al., 1982). Therefore, the recovery half-times for vimentin IF are very similar to those made for the other major cytoskeletal components. It is also interesting that the fluorescence recovery appeared to slow down relative to controls in the presence of MT and MF inhibitors. Therefore, the exchange mechanisms involved in the steady-state turnover of vimentin may depend to some unknown extent on either MT or MF. It is conceivable that in the case of MT, the movement of exchangeable vimentin subunits may be related to the kinesin-based motility of vimentin IF (Gyoeva and Gelfand, 1991) and the recently discovered protofilamentous aggregates of IF protein found in spreading fibroblasts (Prahlad et al., 1998).

Type III IF networks containing vimentin exhibit a remarkable diversity of motile properties that require energy. The majority of these properties appear to reflect interactions with MT, MF, and their associated proteins (see Chou et al., 1997). Only the shape changes exhibited by IF appear to be independent of the other cytoskeletal systems. The mechanism underlying the changes in shape may be related to posttranslational modifications such as phosphorylation/dephosphorylation, which are thought to be involved in regulating the assembly and disassembly of IF (Eriksson et al., 1992; Inagaki et al., 1996). In this regard, it has been hypothesized that the hierarchical structure of IF produces a thermodynamically unstable seam that spirals along their length (Stewart, 1993). It is likely that this seam contains the most readily exchangeable subunits within IF. Perhaps the differential removal or addition of subunits in the region of this seam relative to more rigid regions of the IF wall could account for the changes in the shape of vimentin fibrils in vivo.

In summary, GFP-vimentin fibrils can translocate, appear, or disappear within short time intervals, alter their shapes, and apparently alter their lengths. The significance of these motile properties of IF remains unknown. However, the surprisingly complex and continuous movements of intermediate filaments raise interesting new questions regarding their functions and their interactions with other cytoskeletal systems.

References

Alber, K., and E. Fuchs. 1989. Expression of mutant keratin cDNAs in epithelial cells reveals possible mechanisms for initiation and assembly of intermediate filaments. *J. Cell Biol.* 108:1477–1493.

Aubin, J.E., M. Osborn, W.W. Franke, and K. Weber. 1980. Intermediate filaments of the vimentin-type and the cytokeratin-type are distributed differently during mitosis. *Exp. Cell Res.* 129:149–165.

Brown, A., G. Bernier, M. Mathieu, J. Rossant, and R. Kothary. 1995. The mouse dystonia musculorum gene is a neural isoform of bullous pemphigoid antigen 1. *Nat. Genet.* 10:301–306.

Chou, Y.H., J.R. Bischoff, D. Beach, and R.D. Goldman. 1990. Intermediate filament reorganization during mitosis is mediated by p34cdc2 phosphorylation of vimentin. *Cell.* 62:1063–1071.

Chou, Y.H., P. Opal, R.A. Quinlan, and R.D. Goldman. 1996. The relative roles of specific N- and C-terminal phosphorylation sites in the disassembly of intermediate filament in mitotic BHK-21 cells. *J. Cell Sci.* 109:817–826.

Chou, Y.H., O. Skalli, and R.D. Goldman. 1997. Intermediate filaments and cytoplasmic networking: new connections and more functions. *Curr. Opin. Cell Biol.* 9:49–53.

Collier, N.C., M.P. Sheetz, and M.J. Schlesinger. 1993. Concomitant changes in mitochondria and intermediate filaments during heat shock and recovery of chicken embryo fibroblasts. *J. Cell Biochem.* 52:297–307.

Cubitt, A.B., R. Heim, S.R. Adams, A.E. Boyd, L.A. Gross, and R.Y. Tsien. 1995. Understanding, improving and using green fluorescent proteins. *Trends Cell Biol.* 20:448–455.

Donaldson, J.G., J. Lippincott-Schwartz, G.S. Bloom, T.E. Kreis, and R.D. Klausner. 1990. Dissociation of a 110-kD peripheral membrane protein from the Golgi apparatus is an early event in brefeldin A action. *J. Cell Biol.* 111: 2295–2306.

Eriksson, J.E., D.L. Brautigan, R. Vallee, J. Olmsted, H. Fujiki, and R.D. Goldman. 1992. Cytoskeletal integrity in interphase cells requires protein phosphatase activity. *Proc. Natl. Acad. Sci. USA.* 89:11093–11097.

Evan, G.I., G.K. Lewis, G. Ramsay, and J.M. Bishop. 1985. Isolation of monoclonal antibodies specific for human c-myc proto-oncogene product. *Mol. Cell. Biol.* 5:3610–3616.

Fischer, M., S. Kaech, D. Knutti, and A. Matus. 1998. Rapid actin-based plasticity in dendritic spines. *Neuron.* 20:847–854.

Franke, W.W., E. Schmid, C. Grund, and B. Geiger. 1982. Intermediate filament proteins in nonfilamentous structures: transient disintegration and inclusion of subunit proteins in granular aggregates. *Cell.* 30:103–113.

Goldman, R.D., and D.M. Knipe. 1973. Functions of cytoplasmic fibers in nonmuscle cell motility. *Cold Spring Harbor Symp. Quant. Biol.* 37:523–534.

Gorbsky, G.J., and G.G. Borisy. 1989. Microtubules of the kinetochore fiber turn over in metaphase but not in anaphase. *J. Cell Biol.* 109:653–662.

Gyoeva, F.K., and V.I. Gelfand. 1991. Co-alignment of vimentin intermediate filaments with microtubules depends on kinesin. *Nature.* 353:445–448.

Hirokawa, N., S. Hisanaga, and Y. Shiomura. 1988. MAP2 is a component of crossbridges between microtubules and neurofilaments in the neuronal cytoskeleton: quick-freeze, deep-etch immunoelectron microscopy and reconstitution studies. *J. Neurosci.* 8:2769–2779.

Hollenbeck, P.J., A.D. Bershadsky, O.Y. Pletjushkina, I.S. Tint, and J.M. Vasiliev. 1989. Intermediate filament collapse is an ATP-dependent and actin-dependent process. *J. Cell Sci.* 92:621–631.

Ho, C.-L., J.L. Martys, A. Mikhailov, G.G. Gundersen, and R.K.H. Liem. 1998. Novel features of intermediate filament dynamics revealed by green fluorescent protein chimeras. *J. Cell Sci.* 111:1767–1778.

Inagaki, M., Y. Matsuoka, K. Tsujimura, S. Ando, T. Tokui, T. Takahashi, and N. Inagaki. 1996. Dynamic properties of intermediate filaments: regulation by phosphorylation. *Bioessay.* 18:481–487.

Jones, S.M., J.C.R. Jones, and R.D. Goldman, 1988. Fractionation of desmosomes and comparison of the polypeptide composition of desmosomes prepared from two bovine epithelial tissues. *J. Cell. Biochem.* 36:223–236.

Klymkowsky, M.W. 1981. Intermediate filaments in 3T3 cells collapse after intracellular injection of a monoclonal anti-intermediate filament antibody. *Nature.* 291:249–251.

Kreis, T.E., B. Geiger, and J. Schlessinger. 1982. Mobility of microinjected rhodamine actin within living chicken gizzard cells determined by fluorescence photobleaching recovery. *Cell.* 29:835–845.

Laemmli, U.K. 1970. Cleavage of structural proteins during the assembly of the head of bacteriophage T4. *Nature.* 227:680–685.

Liao, G., T. Nagasaki, and G.G. Gundersen. 1995. Low concentrations of nocodazole interfere with fibroblast locomotion without significantly affecting microtubule level: implications for the role of dynamic microtubules in cell locomotion. *J. Cell Sci.* 108:3473–3483.

Ludin, B., and A. Mauts. 1998. GFP illuminates the cytoskeleton. *Trends Cell Biol.* 8:72–77.

McKenna, N.M., and Y.L. Wang. 1986. Possible translocation of actin and alpha-actinin along stress fibers. *Exp. Cell Res.* 167:95–105.

McLean, W.H., L. Pulkkinen, F.J. Smith, E.L. Rugg, E.B. Lane, F. Bullrich, R.E. Burgeson, S. Amano, D.L. Hudson, K. Owaribe, J.A. McGrath, J.R. McMillan, R.A. Eady, I.M. Leigh, A.M. Christiano, and J. Uitto. 1996. Loss of plectin causes epidermolysis bullosa with muscular dystrophy: cDNA cloning and genomic organization. *Gene Dev.* 10:1724–1735.

Miller, R.K., S. Khuon, and R.D. Goldman. 1993. Dynamics of keratin assembly: exogenous Type I keratin rapidly associates with Type II keratin in vivo. *J. Cell Biol.* 122:123–135.

Mitchison, T.J. 1989. Polewards microtubule flux in the mitotic spindle: evidence from photoactivation of fluorescence. *J. Cell Biol.* 109:637–652.

Ngai, J., T.R. Coleman, and E. Lazarides. 1990. Localization of newly synthesized vimentin subunits reveals a novel mechanism of intermediate filament assembly. *Cell.* 60:415–427.

Okabe, S., H. Miyasaka, and N. Hirokawa. 1993. Dynamics of the neuronal intermediate filaments. *J. Cell Biol.* 121:375–386.

Olson, K.R., J.R. McIntosh, and J.B. Olmsted. 1995. Analysis of MAP 4 function in living cells using green fluorescent protein (GFP) chimeras. *J. Cell Biol*. 130:639–650.

Osborn, M., W. Franke, and K. Weber. 1980. Direct demonstration of the presence of two immunologically distinct intermediate-sized filament systems in the same cell by double immunofluorescence microscopy. Vimentin and cytokeratin fibers in cultured epithelial cells. *Exp. Cell Res*. 125:37–46.

Prahlad, V., M. Yoon, R.D. Moir, R.D. Vale, and R.D. Goldman. 1998. Rapid movements of vimentin on microtubule tracks: kinesin dependent assembly of Intermediate Filament networks. *J. Cell Biol*. 143:159–170.

Rosevear, E.R., M. McReynolds, and R.D. Goldman. 1990. Dynamic properties of intermediate filaments: disassembly and reassembly during mitosis in baby hamster kidney cells. *Cell Motil. Cytoskelet*. 17:150–166.

Saxton, W.M., D.L. Stemple, R.J. Leslie, E.D. Salmon, M. Zavortink, and J.R. McIntosh. 1984. Tubulin dynamics in cultured mammalian cells. *J. Cell Biol*. 99:2175–2186.

Schliwa, M., and J. van Blerkom. 1981. Structural interaction of cytoskeletal components. *J. Cell Biol*. 90:222–235.

Soellner, P., R.A. Quinlan, and W.W. Franke. 1985. Identification of a distinct soluble subunit of an intermediate filament protein: tetrameric vimentin from living cells. *Proc. Natl. Acad. Sci. USA*. 82:7929–7933.

Steinert, P.M., W.W. Idler, and S.B. Zimmerman. 1976. Self-assembly of bovine epidermal keratin filaments in vitro. *J. Mol. Biol*. 108:547–567.

Stewart, M. 1993. Intermediate filament structure and assembly. *Curr. Opin. Cell Biol*. 5:3–11.

Svitkina, T.M., A.B. Verkhovsky, and G.G. Borisy. 1996. Plectin sidearms mediate interaction of intermediate filaments with microtubules and other components of the cytoskeleton. *J. Cell Biol*. 135:991–1007.

Towbin, H., T. Staehelin, and J. Gordon. 1979. Electrophoretic transfer of proteins from polyacrylamide gels to nitrocellulose sheets: procedure and some applications. *Proc. Natl. Acad. Sci. USA*. 76:4350–4354.

Vasquez, R.J., B. Howell, A.M. Yvon, P. Wadsworth, and L. Cassimeris. 1997. Nanomolar concentrations of nocodazole alter microtubule dynamic instability in vivo and in vitro. *Mol. Biol. Cell*. 8:973–985.

Vikstrom, K.L., G.G. Borisy, and R.D. Goldman. 1989. Dynamic aspects of intermediate filament networks in BHK-21 cells. *Proc. Natl. Acad. Sci. USA*. 86:549–553.

Vikstrom, K.L., S.S. Lim, R.D. Goldman, and G.G. Borisy. 1992. Steady state dynamics of intermediate filament networks. *J. Cell Biol*. 118:121–129.

Wang, Y.L. 1985. Exchange of actin subunits at the leading edge of living fibroblasts: possible role of treadmilling. *J. Cell Biol*. 101:597–602.

Waterman-Storer, C.M., and E.D. Salmon. 1997. Actomyosin-based retrograde flow of microtubules in the lamella of migrating epithelial cells influences microtubule dynamic instability and turnover and is associated with microtubule breakage and treadmilling. *J. Cell Biol*. 139:417–434.

Yang, H.Y., N. Lieska, A.E. Goldman, and R.D. Goldman. 1985. A 300,000-mol-wt intermediate filament-associated protein in baby hamster kidney (BHK-21) cells. *J. Cell Biol*. 100:620–631.

Yang, H.Y., N. Lieska, A.E. Goldman, and R.D. Goldman. 1992. Colchicine-sensitive and colchicine-insensitive intermediate filament systems distinguished by a new intermediate filament-associated protein, IFAP-70/280 kD. *Cell Motil. Cytoskelet*. 22:185–199.

Yang, Y., J. Dowling, Q.C. Yu, P. Kouklis, D.W. Cleveland, and E. Fuchs. 1996. An essential cytoskeletal linker protein connecting actin microfilaments to intermediate filaments. *Cell*. 86:6556–6565.

Zackroff, R.V., and R.D. Goldman. 1979. In vitro assembly of intermediate filaments from baby hamster kidney (BHK-21) cells. *Proc. Natl. Acad. Sci. USA*. 76:6226–6230.